Shifting foci of hematopoiesis during reconstitution from single stem cells

Yu-An Cao*†, Amy J. Wagers†‡, Andreas Beilhack§, Joan Dusich*, Michael H. Bachmann*, Robert S. Negrin§, Irving L. Weissman‡, and Christopher H. Contag*¶

Departments of *Pediatrics, ‡Pathology, and §Medicine, Stanford University School of Medicine, Stanford, CA 94305

Contributed by Irving L. Weissman, October 29, 2003

To reveal the early events and dynamics of hematopoietic reconstitution in living animals in real-time, we used bioluminescence imaging to monitor engraftment from single luciferase-labeled hematopoietic stem cells (HSC) in irradiated recipients. Transplanted HSC generated discrete foci in the spleen and bone marrow (BM), at a frequency that correlated with BM compartment size. Initially detected foci could expand locally, seed other sites in BM or spleen, and/or recede with different kinetics. These studies reveal dynamic and variable patterns of engraftment from highly purified HSC and indicate that the final overall contribution of individual HSC to hematopoietic chimerism does not depend on the specific site of initial engraftment and expansion.

Stem cells hold tremendous potential for cancer therapy, tissue engineering, and cellular therapeutics. Understanding stem cell behavior and biology in the context of the living body, where the influences of tissue and organ systems remain intact, is essential for successful development of stem cell-based therapies. Hematopoietic stem cells (HSC) are well characterized, self-renewing, multipotent cells that can produce lifelong, complete hematopoietic reconstitution (1, 2). HSC function has been studied from a variety of experimental approaches, but HSC function typically must be assayed once tissues are removed from the body, often weeks or months after transplantation. Yet the critical early events of homing to the spleen and bone marrow (BM), seeding in the stromal microenvironment, and initial expansion of short- and long-term reconstituting cells occur within the first hours to days after transplantation (3–8) and are therefore inaccessible to investigation in most studies. We have previously described an *in vivo* bioluminescence imaging (BLI) method to elucidate the spatiotemporal trafficking patterns of malignant cells, lymphocytes, and other mature immune cells within living animal models of human biology and disease (9–12). This technology utilizes low-light imaging systems based on charge-coupled device cameras to detect luminescent signals that emanate from within the body from cells expressing the enzyme luciferase. For BLI detection of luciferase activity in living animals, the substrate for luciferase, luciferin, is administered i.v. or i.p. and rapidly diffuses throughout all tissues and enters many cell types. The level of photon emission and the spectrum of emitted light from luciferase-expressing mammalian cells is adequate to penetrate the tissues of small research animals, such as mice and rats, and thus can be detected externally with low-light imaging cameras (9–12). Here we apply this method to study the early events and dynamics of engraftment following transplantation of small numbers of highly purified, syngeneic mouse HSC into lethally irradiated recipients.

Materials and Methods

Animals. The luciferase transgenic mouse line (FVB.luc$^+$), expressing firefly luciferase under the control of the widely expressed β-actin promoter, was made by pronuclear injection of the reporter gene construct in the transgenic animal facility in the Department of Pathology at Stanford University (Y.-A.C., unpublished data). FVB.luc$^+$ mice express various levels of luciferase activity in all leukocyte subsets tested, including CD4$^+$ and CD8$^+$ T cells, B220$^+$ B cells, NK1.1$^+$ natural killer cells, and Gr-1$^+$Mac-1$^+$ granulocytes, as well as hematopoietic stem and progenitor cells; luciferase activity was not detected at significant levels in mature erythrocytes (Ter119$^+$CD45$^-$), but low levels of activity were detectable in erythrocyte precursors (Y.-A.C., unpublished data; Figs. 5 and 6, which are published as supporting information on the PNAS web site, and data not shown). FVB.Cg-Tg(GFPU)5Nagy mice were purchased from The Jackson Laboratory and bred with FVB.luc$^+$ mice. FVB.Cg-Tg(GFPU)5Nagy mice express GFP driven by the chicken β-actin promoter and cytomegalovirus intermediate early enhancer. GFP is expressed in all tissues of these mice, with the exception of hemoglobin-expressing mature erythrocytes. FVB/NJ recipients (8 to 12 weeks old) were obtained from The Jackson Laboratory and Charles River Breeding Laboratories and irradiated with a 200-kV irradiator (RT250; Philips, Shelton, CT) with a total dose of 900 cGy (450 + 450 cGy) administered in two fractions 3 h apart. All mice were housed in the Research Animal Facility at Stanford University. Recipients were given acidified water before irradiation and antibiotic water (1.1 g/liter neomycin sulfate and 10^6 units/liter polymyxin B sulfate) after irradiation to reduce the chance of infection by opportunistic pathogens. All procedures were approved by the Animal Care and Use Committee of Stanford University.

Antibodies. The antibodies used in these studies included 19XE5 (anti-Thy1.1, phycoerythrin conjugate), 2B8 (anti-c-kit, allophycocyanin conjugate), E13-161.7 (anti-Sca-1, Ly6A/E, Texas red conjugate), and anti-Flk2 (phycoerythrin conjugate; Ebioscience, San Diego). The mixture of lineage marker antibodies included KT31.1 (anti-CD3), GK1.5 (anti-CD4), 53–7.3 (anti-CD5), 53–6.7 (anti-CD8), Ter119 (anti-erythrocyte-specific antigen), 6B2 (anti-B220), 8C5 (anti-Gr-1), and M1/70 (anti-Mac-1). Unless otherwise indicated, all antibodies were produced and purified in the I.L.W. laboratory.

Isolation and Transplantation of Hematopoietic Stem Cells. BM was isolated as described (13). Isolated BM cell suspensions were then filtered through nylon mesh before staining for HSC. Donor c-kit$^+$Thy-1.1^{lo}Lin$^-$Sca-1$^+$ (KTLS) HSC (1, 2) and other multipotent cell populations were isolated by double fluorescence-activated cell sorting (FACS) of c-kit-enriched bone marrow from *luc*$^+$ or *luc*$^+$ GFP$^+$ transgenic mice, based on previously defined reactivity for particular cell surface markers (including lineage markers, c-kit, Thy1.1, Sca-1, and Flk-2) (1, 2, 14, 15). The total HSC population, including long-term (LT)- and short-term (ST)-HSC, was defined by the phenotype c-kit$^+$Thy1.1^{lo}Lin$^{-/lo}$Sca-1$^+$. In experiments designed to compare multipotent hematopoietic cells, LT-HSC were isolated by

Abbreviations: BM, bone marrow; HSC, hematopoietic stem cell; BLI, bioluminescence imaging; KTLS, c-kit$^+$Thy-1.1^{lo}Lin$^-$Sca-1$^+$; LT-HSC, long-term HSC; ST-HSC, short-term HSC; MPP, multipotent progenitor; FACS, fluorescence-activated cell sorting.

†Y.-A.C. and A.J.W. contributed equally to this work.

¶To whom correspondence should be addressed at: Department of Pediatrics, Division of Neonatal and Developmental Medicine, Clark Center, Room 150-B, 318 Campus Drive, Stanford, CA 94305. E-mail: ccontag@cmgm.stanford.edu.

the phenotype c-kit$^+$Thy1.1^{lo}Lin$^{-/lo}$Sca-1$^+$Flk-2$^-$; ST-HSC were isolated by the phenotype c-kit$^+$Thy1.1^{lo}Lin$^{-/lo}$Sca-1$^+$Flk-2$^+$; and multipotent progenitors (MPP) were isolated by the phenotype c-kit$^+$Thy1.1$^-$Lin$^{-/lo}$Sca-1$^+$Flk-2$^+$ (15). Single LT-HSC were isolated as described (13). To ensure purity, all populations were double sorted with a highly modified Vantage SE cell sorter (Becton Dickinson Immunocytometry Systems) provided by the Stanford University Shared FACS Facility. Flow cytometry data were analyzed with FLOJO (Treestar, San Carlos, CA) analysis software. Purified hematopoietic cells were transferred i.v. into irradiated recipient mice by retroorbital injection as described (13). For transfer of 10, 50, or 250 HSC, cells were cotransplanted with 3×10^5 unfractionated host-type (nontransgenic) BM cells. Single LT-HSC were cotransplanted with 3×10^5 Sca-1-depleted BM from nontransgenic donors. Sca-1 depletion was performed as described (13).

Hematopoietic Chimerism Analysis. Chimerism of peripheral blood leukocytes was determined in transplanted mice by flow cytometry as described (13). Because these *luc*$^+$ GFP$^+$ transgenic mice express GFP in only a subset of peripheral blood leukocytes (from ≈10% to 90% depending on cell lineage; data not shown), GFP chimerism of transplanted animals was normalized based on the frequency of GFP expression in peripheral blood leukocytes isolated from unmanipulated *luc*$^+$ GFP$^+$ transgenic animals.

BLI. Bioluminescent images were taken as described (9, 10). Briefly, mice were anesthetized with Avertin (250 μg/kg i.p.) and luciferin was administered at a dose of 150 mg/kg i.p. At the time of imaging, animals were placed in a light-tight chamber, and photons emitted from luciferase expressed in cells from within the animal, and transmitted through the tissue, were collected with integration times of 1–10 min, depending on the intensity of the bioluminescence emission. Images were captured with an *in vivo* imaging system employing a cooled charge-coupled device camera (IVIS; Xenogen, Alameda, CA). Dorsal, ventral, and two lateral images were obtained from each animal at each time point to better determine the origin of photon emission. Further confirmation was obtained in a subset of animals by dissecting the tissues, incubating fresh tissues in D-luciferin, and imaging these tissues without the overlying tissues.

Immunofluorescence Analysis. Tissues of transplanted animals were prepared as described (13). GFP$^+$ donor cells were detected in frozen sections of spleen harvested from recipients of *luc*$^+$ GFP$^+$ HSC 13 days after the transplantation. Eight- to 10-μm frozen sections were cut at −20°C from OCT-embedded tissues with a 5030 series Microtome (Bright Instruments, Huntingdon, England). Sections were air dried overnight at room temperature and then stained. Sections were blocked with a mouse on mouse blocking kit (M.O.M.; Vector Laboratories) and the Avidin/Biotin blocking kit (Vector Laboratories). Serial sections were stained for immunofluorescence with anti-GFP and leukocyte-specific biotinylated primary antibodies (anti-Mac-1, anti-GR-1, or anti-B220). Primary antibodies were detected by using Alexa Fluor 594-conjugated streptavidin (Molecular Probes). Endogenous GFP signals were amplified by staining with Alexa Fluor 488-conjugated anti-GFP polyclonal antibody (Molecular Probes). Nuclei were labeled with Hoechst 33342 (Molecular Probes). Immunofluorescent labeling was analyzed by standard fluorescence microscopy by using a Nikon Eclipse E800 microscope, with epifluorescence powered by a super-high-pressure mercury lamp (Nikon, Tokyo, Japan). Sequential images were acquired with a real-time charge-coupled device camera (SPOT RT CCD; Diagnostic Instruments, Sterling Heights, MI) using UV-2A, HYQ Texas red, and HYQ FITC (Nikon) filters for Hoechst 33342, Alexa Fluor 594, and GFP, respectively, and electronically merged with SPOT RT software (Diagnostic Instruments).

Results

Discrete Foci of Engraftment from Purified HSC. To enable the study of multilineage hematopoietic reconstitution from a small number of HSC, including single HSC, it was essential to have a constitutively labeled cell population and detectable reporter activity in multiple lineages over many cell generations. We therefore developed a "universal donor" transgenic mouse line that expresses firefly luciferase in all tissues by using a well characterized constitutive promoter (β-actin) (Y.-A.C., unpublished data). Luciferase expression, as indicated by a bioluminescent signal, was detectable from isolated KTLS HSC (1, 2), with a photon output of three photons per cell per sec (Figs. 5 and 6), and from most mature hematopoietic cell subsets obtained from this *luc*$^+$ transgenic donor line (Y.-A.C., unpublished data, and *Materials and Methods*). Significant levels of luciferase activity were not detectable in mature erythrocytes, but luciferase activity was detected in erythrocyte precursors (data not shown). To study the pattern and dynamics of HSC engraftment from highly purified HSC, we isolated KTLS HSC from *luc*$^+$ transgenic donor mice by FACS and transplanted 10, 50, or 250 *luc*$^+$ KTLS HSC together with 3×10^5 radioprotective nontransgenic whole BM cells into lethally irradiated nontransgenic, syngeneic recipients. After i.p. injection of the substrate D-luciferin, hematopoietic engraftment of transplanted HSC was detectable in this system as bioluminescent foci and was apparent in all experimental groups (Fig. 1). Bioluminescent foci were detected as early as 6 days after transplantation and most frequently were observed at anatomic sites corresponding to the location of the spleen, skull, vertebrae, femurs, and sternum, as well as from other BM compartments, including the humeri, tibiae, and ribs (Fig. 1*A* and data not shown). Confirmation of tissue origin was obtained by imaging from different views, and in a subset of animals, tissues were dissected and the predicted origin of luciferase activity was confirmed by *in vitro* incubation with D-luciferin (data not shown). Although the liver has been previously identified as a major site of rapid HSC localization after an i.v. transfer of mobilized peripheral blood HSC (16), bioluminescent signals were not detected from regions corresponding to the liver in HSC-transplanted animals, suggesting that any initial seeding of this organ does not lead to productive local engraftment or expansion of HSC or their progeny. Among the engrafted BM compartments, there were no apparent preferential sites for the formation of the earliest appearing bioluminescent foci. Interestingly, the numbers of foci detected in each recipient at each time point were substantially smaller than the number of transplanted HSC (Fig. 7, which is published as supporting information on the PNAS web site), which may suggest that only a limited number of "niches" were competent for HSC engraftment and hematopoietic expansion after lethal irradiation or that seeding of HSC into supportive microenvironments was limited by the efficiency of HSC homing, survival, and/or proliferation. Alternatively, there may have been additional sites of engraftment in these animals, where the levels of reconstitution by donor cells were below detectable limits. However, the observation that the number of initial bioluminescent foci detected increased with increased number of HSC transplanted suggests that this phenomenon relates to the efficiency of HSC homing or other HSC-intrinsic factors (Fig. 7).

Although bioluminescent signal intensity from the spleen steadily increased in most HSC-transplanted mice (Fig. 1*B*), we frequently found that the absolute intensity of individual bioluminescent foci varied over time. Some foci increased in intensity, whereas others decreased. Some foci completely disappeared over the course of the first few days after detection, whereas new ones emerged in the same period (Fig. 1*B*). Regardless of how dramatic the intensity change for individual bioluminescent foci, hematopoietic reconstitution, measured by whole body photon emission, rapidly progressed (Fig. 1*C*). Engraftment from *luc*$^+$ HSC peaked at 6 weeks after transplantation and remained high thereafter. Increasing the

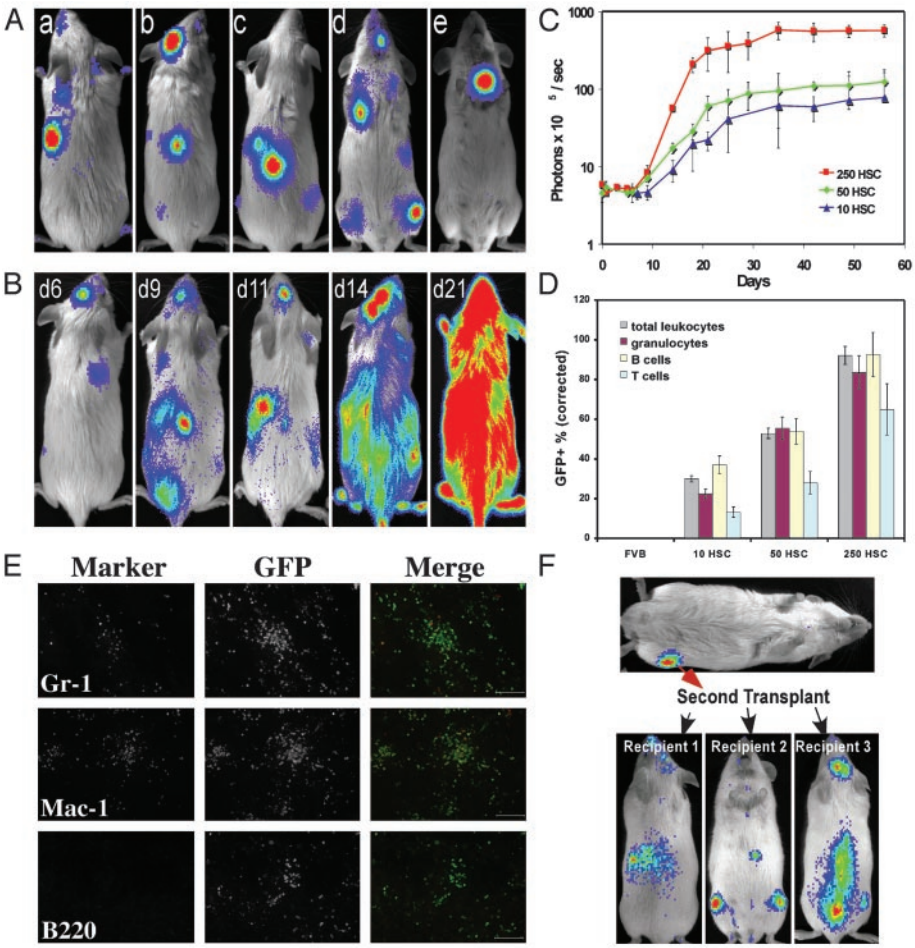

Fig. 1. Dynamics of HSC engraftment from *luc*$^+$ or *luc*$^+$ GFP$^+$ HSC. HSC were sorted from transgenic mice and transplanted into lethally irradiated nontransgenic recipients. BLI was used to monitor the engraftment of HSC. All images are displayed at the same scale. (*A*) Bioluminescent foci derived from 50 transplanted *luc*$^+$ HSC were apparent in individual animals at anatomic sites corresponding to the location of the spleen, skull, vertebrae, femurs, and sternum (*a* to *e*, respectively) at 6–9 days after transfer. (*B*) The patterns of engraftment were dynamic with formation and expansion or formation and loss of the bioluminescent foci. One recipient of 250 HSC monitored over time is shown. In this animal, two initial foci were apparent on day 6. By day 9, one was no longer detectable and another remained at nearly the same intensity as on day 6. New foci were apparent on day 9, and then the intensity at these sites weakened or disappeared by day 11. The intensity of the spleen signal increased steadily. By day 21, a significant degree of engraftment had been achieved. (*C*) Dynamics of the hematopoietic engraftment from 10, 50, or 250 *luc*$^+$ or *luc*$^+$ GFP$^+$ HSC. HSC were transplanted along with 3×10^5 whole BM cells from nontransgenic donors, and the dorsal view whole body bioluminescence emission was measured at different time points. Each time point is represented by at least four animals, and data were obtained from dorsal view whole body imaging and are plotted as photons per sec per mouse. (*D*) Engraftment of hematopoietic lineages was determined by flow cytometric analysis of peripheral blood at 8 weeks after transplant of 10, 50, or 250 *luc*$^+$ GFP$^+$ HSC. Peripheral blood cells of wild-type FVB mice (FVB) were analyzed in parallel as a negative control. Data are presented as the mean percent GFP$^+$ cells for the indicated subsets and are corrected for GFP transgene expression as described in *Materials and Methods*. (*E*) Immunofluorescence analysis of spleens recovered from *luc*$^+$ GFP$^+$ HSC-transplanted animals exhibiting splenic bioluminescent foci-revealed clusters of GFP$^+$ mature myeloid cells expressing the markers Mac-1 and Gr-1. (Scale bar = 100 μm.) (*F*) Whole BM from the bioluminescent femur of a recipient of 250 *luc*$^+$ HSC was harvested on day 12 and transplanted into irradiated secondary nontransgenic recipients who subsequently showed detectable engraftment by *luc*$^+$ cells in multiple BM compartments and in the spleen on day 14.

dose of *luc*$^+$ HSC from 10 to 250 did not significantly shorten the time required to reach the peak of the *luc*$^+$ donor-derived engraftment but did increase their overall hematopoietic contribution (Fig. 1*C*). To extend these studies, we crossed *luc*$^+$ transgenic mice with FVB.Cg-Tg(GFPU)5Nagy mice, in which hematopoietic cells are labeled by expression of GFP, which is also driven by the β-actin promoter. We then repeated the study shown in Fig. 1 this time using *luc*$^+$ GFP$^+$ HSC from *luc*$^+$ GFP$^+$ double transgenic animals to allow flow cytometric and fluorescence microscopic analyses of cells and tissues from the recipient mice. The bioluminescence images from these animals revealed the same kinetics of engraftment as observed in the study using *luc*$^+$ HSC (data not shown), and flow cytometric analysis of peripheral blood demonstrated reconstitution of both myeloid and lymphoid lineages in these mice (Fig. 1*D*).

Bioluminescent foci in HSC-transplanted animals likely represent local proliferation and differentiation of *luc*$^+$ HSC and their progeny. To further investigate the cellular composition of the bioluminescent foci, we killed animals that received *luc*$^+$ GFP$^+$ KTLS HSC, removed spleens that showed detectable bioluminescent foci, and analyzed the donor cell contribution at this site by flow cytometry and fluorescence microscopy. Thirteen days after transplantation, fluorescence microscopy revealed the presence in the spleen of discrete colonies of GFP$^+$ cells, the majority of which were composed of myeloid cells expressing the cell surface markers Mac-1 and/or Gr-1 (Fig. 1*E*). Flow cytometric analysis confirmed the presence of significant numbers of donor-derived myeloid cells in both the spleen and BM at sites in which bioluminescent signals were detected (Fig. 8, which is published as supporting information on the PNAS web site). In some cases, phenotypically defined

KTLS HSC were also among the GFP$^+$ cells detected by flow cytometry in spleen and BM exhibiting bioluminescent foci (Fig. 8). To test functionally for the presence of bona fide HSC within these foci, on day 12 we serially transplanted cells harvested from spleens or BM of mice previously transplanted with *luc*$^+$ HSC in which bioluminescent foci were detected. Consistent with HSC maintenance in expanding hematopoietic foci, recipients of secondary cell transplants likewise exhibited engraftment by *luc*$^+$ hematopoietic cells (Fig. 1*F* and data not shown).

Equivalent Patterns of Engraftment and Differential Potential for Expansion of Multipotent Hematopoietic Populations. In mice, the most primitive subset of self-renewing HSC is termed long-term reconstituting HSC (LT-HSC) (c-kit$^+$Thy1.1^{lo}Lin$^{-/lo}$Sca-1$^+$Flk-2$^-$) (2, 15). LT-HSC give rise to ST-HSC (c-kit$^+$Thy1.1^{lo}Lin$^{-/lo}$Sca-1$^+$Flk-2$^+$), which maintain multipotency but show restricted self-renewal potential; ST-HSC give rise to non-self-renewing MPP (c-kit$^+$Thy1.1$^-$Lin$^{-/lo}$Sca-1$^+$Flk-2$^+$) (2, 15). To follow in real time the engraftment properties of multipotent hematopoietic cell populations exhibiting distinct self-renewal and proliferative potential during hematopoietic reconstitution, 500 FACS-purified *luc*$^+$ LT-HSC, ST-HSC, or MPP (Fig. 5) were transplanted into lethally irradiated nontransgenic recipients together with 3×10^5 unlabeled, nontransgenic whole BM cells. BLI revealed bioluminescent foci in all recipients of LT-HSC, ST-HSC, or MPP at early stages of reconstitution and indicated that spleen, vertebrae, skull, and femurs were the most common initial sites of engraftment for all three cell populations. Fewer foci were formed after transplantation of MPP, and MPP-derived foci were weaker in intensity when compared with those formed from LT- or ST-HSC (Fig. 2*A*). The decreased number of foci formed from MPP may reflect a relatively lower seeding efficiency of these cells, or the decreased number of foci may suggest some heterogeneity in engraftment potential within this population. Consistent with previously described differences in the self-renewal potential of these multipotent populations (2, 15), the kinetics of engraftment by each population differed (Fig. 2*B*). Bioluminescent signal derived from transplanted LT-HSC reached a plateau at about week 8 and remained high over the next 100 days. Engraftment by ST-HSC peaked at about 6 weeks after transplantation and subsequently decreased. Recipients of MPP showed low levels of overall reconstitution and a peak signal at week 4, which decreased thereafter (Fig. 2*B*). Luciferase assays of myeloid or lymphoid cells sorted from recipient mice at 15 weeks after transplantation showed sustained multilineage contributions from donor cells in seven of seven LT-HSC-transplanted animals; however, only four of nine ST-HSC- and zero of five MPP-transplanted animals maintained detectable multilineage chimerism at this time point (Fig. 2*C* and data not shown). Animals that received *luc*$^+$ GFP$^+$ LT-HSC, ST-HSC, and MPP showed reconstitution dynamics identical to those receiving *luc*$^+$ HSC. Flow cytometric analysis of cells from these animals at 8 weeks after transplantation showed that ≈65% or 2% of hematopoietic cells were derived from GFP$^+$ HSC or MPP, respectively, and lineage profiles of these GFP$^+$ hematopoietic cells in the peripheral blood of recipient mice revealed lymphoid chimerism at all time points in recipients of LT-HSC, ST-HSC, and MPP. However, only recipients of LT- or ST-HSC maintained chimerism in the myeloid cell lineage at 8 weeks after transplantation (Fig. 9, which is published as supporting information on the PNAS web site). Taken together, these data demonstrate that, although LT-HSC, ST-HSC, and MPP differ in their overall proliferative potential, they show equivalent patterns of homing and engraftment.

No Predisposition for Homing and Engraftment Within Particular BM Compartments. In recipients of multiple HSC, the distribution and expansion of bioluminescent foci varied over time from transplant to full engraftment. Some bioluminescent foci completely disappeared in a couple of days, and others arose late at sites distinct

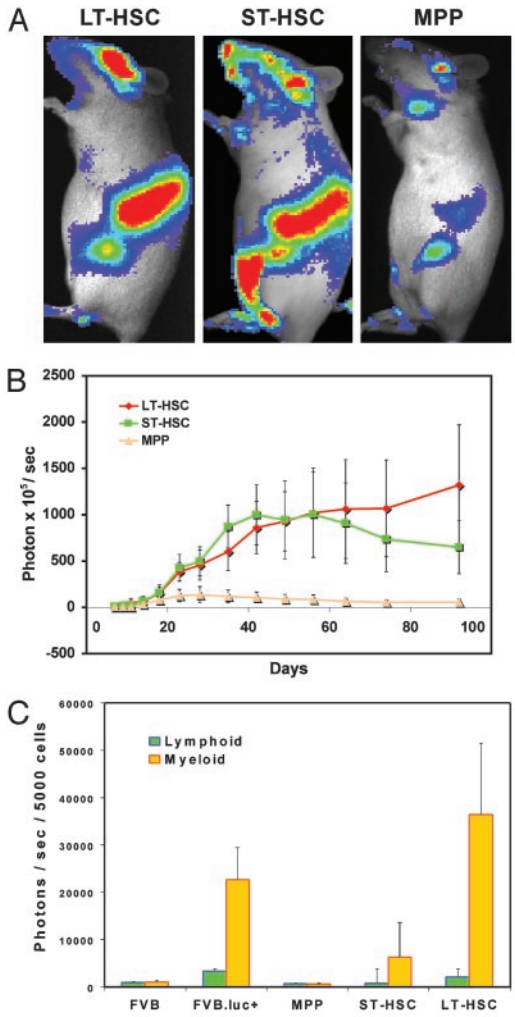

Fig. 2. Engraftment kinetics of different populations of HSC. Five hundred *luc*$^+$ LT-HSC, ST-HSC, or MPP were transplanted into lethally irradiated nontransgenic recipients along with 3×10^5 nontransgenic whole BM cells. BLI was performed at different time points. (*A*) Images were taken on day 18 after transplantation and are displayed at the same scale. The most active tissues for hematopoietic reconstitution were spleen, vertebrae, skull, and femur in all groups. (*B*) Kinetics of LT-HSC, ST-HSC, and MPP engraftment. Values were obtained from dorsal view whole body imaging and are plotted as photons per sec per mouse. Data are plotted as the mean (±SD) for the entire group ($n = 7$ for LT-HSC, $n = 9$ for ST-HSC, and $n = 5$ for MPP). (*C*) Lineage analysis of hematopoietic engraftment. *luc*$^+$ LT-HSC, ST-HSC, or MPP were transplanted into recipient mice, and, 15 weeks after transplantation, mature lymphoid (B220$^+$ or CD3$^+$) or myeloid (Mac-1$^+$Gr-1$^+$) cells were sorted by FACS from the peripheral blood for luciferase assay. Data are plotted as the average (±SD) bioluminescent signal from duplicate assays for seven LT-HSC, nine ST-HSC, and five MPP recipients. Cells from wild-type FVB (FVB) and *luc*$^+$ transgenic (FVB.luc$^+$) mice were analyzed in parallel as negative or positive controls, respectively. Multilineage (myeloid plus lymphoid) chimerism was maintained in seven of seven LT-HSC-, four of nine ST-HSC-, and zero of five MPP-transplanted animals.

from the original foci. It was not clear whether these newly arising bioluminescent foci were derived from migrating stem/progenitor cells that came from the original foci or whether these foci represented sites of engraftment in which HSC exhibited an initial dormancy or delayed expansion after BM homing. Single HSC, by definition, can engraft initially at only one site; therefore, any bioluminescent foci that emerge in single HSC-transplanted mice at a later time point must arise by migration of an HSC and/or its progeny to a new location. Thus, single HSC-reconstituted mice

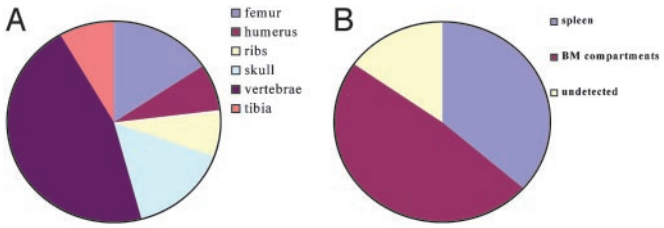

Fig. 3. Frequent locations of original bioluminescent foci derived from single HSC. Single *luc*$^+$ or *luc*$^+$ GFP$^+$ KTLS HSC were transplanted into lethally irradiated nontransgenic recipients along with 3×10^5 nontransgenic Sca-1$^-$ BM cells. BLI was performed on day 12–23 after transplantation, and at these time points, single bioluminescent foci were visualized from 23 of a total of 113 recipients at different time points; four recipients showed no single bioluminescent foci on days 12–23 but did show detectable levels of hematopoietic engraftment after 4 weeks and therefore were categorized as undetected at the early time point. (*A*) Frequent sites among different BM compartments where bioluminescent foci were initially detected. (*B*) The frequency of bioluminescent foci detected from spleen or BM compartments.

allow a more refined determination of the frequency and dynamics of hematopoietic reconstitution. In addition, in these animals, we can track "nonproductive" engraftments that lead to transient but not long-term reconstitution to potentially correlate such events with distinct anatomical locations of engraftment.

We therefore transplanted single *luc*$^+$ GFP$^+$ KTLS HSC along with 3×10^5 Sca-1-depleted BM cells (13) into lethally irradiated recipients and tracked the animals by using BLI. In animals that received a single *luc*$^+$ KTLS HSC, we first observed single bioluminescent foci by 12–23 days in ≈20% of recipients (23 of a total of 113 recipients transplanted). In four recipients, initial foci were not detected at 12–23 days after transplantation, but detectable levels of hematopoietic engraftment were apparent at later time points (data not shown). Among different BM compartments, vertebrae were the most frequent location where initial bioluminescent foci were detected, followed by skull, femur, humeri, ribs, and tibiae (Fig. 3*A*). These data are consistent with those from multiple HSC transplants and correlate well with the estimated size of BM compartments in normal animals, which indicates that vertebrae represent the largest BM compartment (17). This correlation suggests that HSC may randomly home to and engraft available "niches" in different BM compartments with no predisposition for homing or engraftment at particular locations. In these experiments, about 37% of original bioluminescent foci were detected from spleen (Fig. 3*B*), suggesting that the spleen is the most frequent site initially engrafted in lethally irradiated animals by transplanted HSC. The large proportion of initial bioluminescent signals detected from the spleen after transplantation likely reflects the conversion of this organ from a predominantly lymphoid tissue into a more hematopoietically active one after myeloablation.

Different Outcomes from Initial Engraftment of Single HSC. We followed each of the single HSC recipients exhibiting initial bioluminescent foci and found that the fates of these single foci could differ dramatically. In reconstituted animals, some foci demonstrated increasing intensity over time as evidence of expansion that led to a high overall level of hematopoietic reconstitution (Fig. 4 *A*, *B*, and *C*), whereas the intensity of other foci lessened over time and yielded only a very low level engraftment (Fig. 4*D*). Some foci became undetectable a couple of weeks after initial detection. In one representative case, where a single HSC produced high-level reconstitution, local photon emission from the original focus consistently increased from the time of initial detection until week 3 and

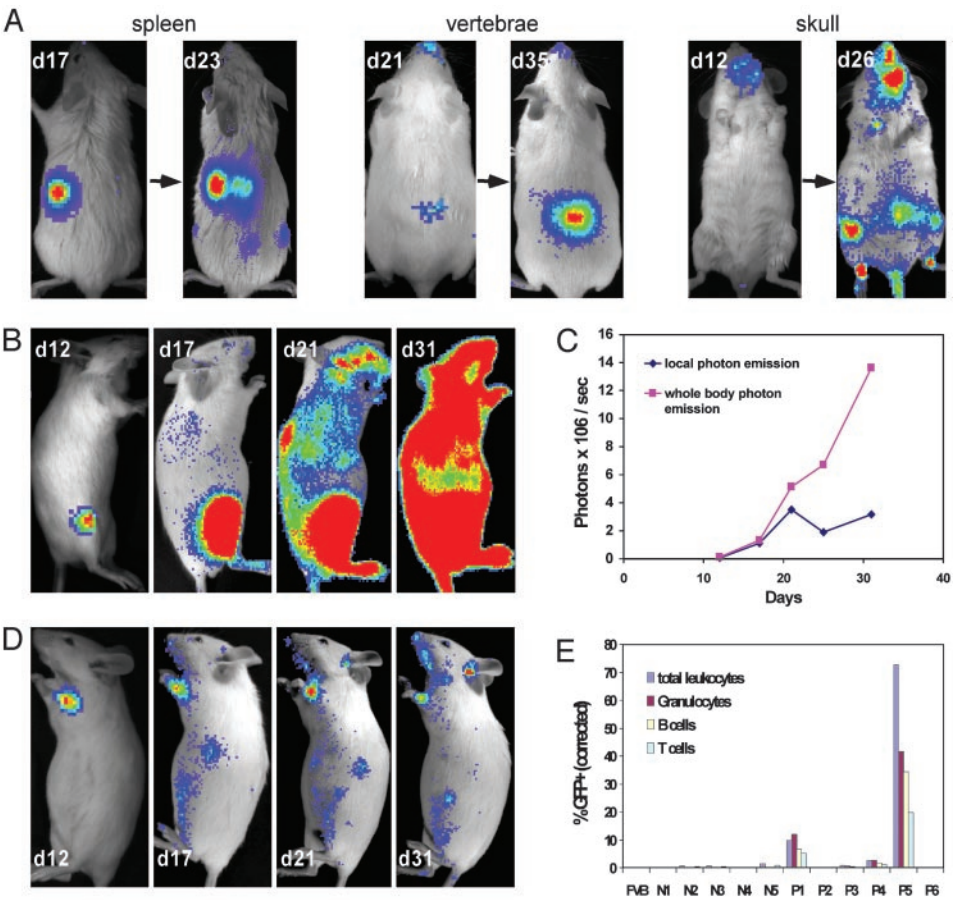

Fig. 4. Single HSC engraftment. Single *luc*$^+$ or *luc*$^+$ GFP$^+$ KTLS HSC were injected i.v. into lethally irradiated FVB recipients along with 3×10^5 Sca-1-depleted BM cells as a radioprotective population. All images are displayed at the same scale. (*A*) Representative images showing single HSC-engrafted mice in which single foci from spleen, vertebrae, and skull were observed. These foci expanded with time, and new detectable sites became apparent at later time points. (*B*) Right lateral view images were taken on days 12, 17, 21, and 31 from one animal in which one initial bioluminescent focus was visualized on day 12 after transplantation. By day 31, a significant degree of hematopoietic reconstitution was apparent. (*C*) Kinetics of hematopoietic reconstitution of the recipient shown in *B* showed steady increases in whole body bioluminescent emission with relatively stable signal detected from the initial focus (local photon emission). (*D*) One focus from another single HSC recipient yielded only low-level hematopoietic engraftment. Left lateral view images were taken on days 12, 17, 21, and 31. (*E*) Chimerism evaluation of peripheral blood of the single *luc*$^+$ GFP$^+$ HSC recipients in a representative experiment, including wild-type FVB and recipients with (P1–6) and without (N1–5) initial foci. At week 5, 72.7% of hematopoietic cells from P5 (recipient shown in *B*) were derived from donor HSC, whereas only 0.3% of those from P6 (recipient shown in *D*) were derived from the labeled donor cell.

then fluctuated from week 4; whole body photon emission continued to increase and reached a plateau at ≈week 5 (Fig. 4 *B* and *C*). The initial site of focus formation (spleen or BM) did not appear to affect the ultimate level of hematopoietic reconstitution achieved, because whole body bioluminescent signals measured at week 8 from single HSC-engrafted animals whose initial BL signal was detected (on day 12–23) in either spleen or BM did not differ significantly from each other (data not shown). Moreover, initial engraftment of single HSC in identical compartments of different recipient mice did not lead to equivalent contributions to hematopoietic reconstitution. Although the precise mechanism(s) underlying such differences in outcome following single HSC engraftment are currently unknown, these may include differences in the ability of particular microenvironments within the BM to promote hematopoietic expansion or may suggest that some specific heterogeneity in the KTLS HSC population, such as differences in HSC cell cycle status, can affect the ability of these cells to engraft and be maintained at particular locations.

The kinetics of hematopoietic engraftment by single HSC were slightly delayed compared with those seen on transplantation of higher numbers (500) of purified HSC, and initial foci generally were not detectable until 12–23 days after transplantation. However, in many of these mice, new foci subsequently arose at locations distant from the initial sites of engraftment, including the spleen (data not shown) and other BM compartments (Fig. 4 *A* and *B*). Even in cases where transplanted single HSC produced only a low overall level of reconstitution, new foci were also visualized arising at later time points from the spleen and BM (Fig. 4*D* and data not shown). We confirmed multilineage (both lymphoid and myeloid) hematopoietic engraftment of single *luc*$^+$ GFP$^+$ KTLS HSC-reconstituted mice by flow cytometric analysis of peripheral blood (Fig. 4*E*). As reported in previous studies (13), the overall level of hematopoietic reconstitution from single HSC varied, but in some recipients, donor cell chimerism reached levels as high as 72.7% (Fig. 4*E*). Thus, these data suggest that during hematopoietic reconstitution from transplanted cells, HSC first proliferate and differentiate locally in their initial site of engraftment and subsequently expand to engraft additional distinct locations at later stages of reconstitution. The emergence of secondary foci at locations distant from the original site of engraftment likely indicates that this expansion is mediated through migration of HSC and/or their progeny through the bloodstream during the process of hematopoietic reconstitution.

Discussion

By using this *in vivo* imaging approach we find that after irradiation and transplantation, hematopoietic cell reconstitution originates first from a limited number of hematopoietic foci in the spleen and/or BM. Additional marrow or splenic sites are seeded at later time points after the migration of HSC or their progeny from the original focus. Different BM compartments appear equivalent for initial engraftment of HSC, because the frequency with which particular BM compartments are seeded correlates roughly with compartment size. In addition, the observation that the number of initial foci detected from transplanted HSC, although increasing with increasing HSC dose, is not equal to the number of transplanted HSC suggests that hematopoietic engraftment is likely determined by the efficiency of HSC homing or by other HSC-intrinsic factors. However, it is also possible that the precise locations in which particular HSC may land can differ in their ability to support HSC expansion and differentiation, such that only a fraction of transferred cells reach supportive environments where they are capable of generating bioluminescent foci. Nonetheless, the final overall contribution of individual HSC to hematopoietic chimerism does not appear to depend on whether initial engraftment occurs in the spleen or in the BM, and successful initial engraftment of individual HSC at a particular site does not ensure maintenance of hematopoiesis at that site. Finally, LT-HSC, ST-HSC, and MPP show equivalent patterns of homing and engraftment but differ in their overall proliferative potential, suggesting that intrinsic differences in self-renewal potential, rather than differences in migration, underlie the differences in reconstitution capacity of these multipotent cell populations. These findings are consistent with and extend those recently reported by Wang *et al.* (18), who used BLI to investigate hematopoietic engraftment by luciferase-expressing human stem and progenitor cells in a NOD/SCID/β2m^{null} xenotransplant model. These investigators likewise observed strong bioluminescent signals from engrafted human cells in multiple BM compartments and found kinetic differences in engraftment after the transplantation of CD34$^+$ or more primitive CD34$^+$CD38$^-$ umbilical cord blood cells.

The imaging strategy described here offers a powerful approach for studying hematopoietic cells under physiological conditions where the contextual influences of intact organ systems can be evaluated. Because different mouse strains have different genetically determined frequencies of HSC in BM (19, 20), the establishment and expansion of genetically distinct HSC populations *in vivo* in real time might be best studied with these noninvasive techniques. Further, there exist in allogeneic hosts T cell and natural killer cell barriers to HSC transplants (21), although these are not evident as direct killing of HSC by natural killer cells (22). It would be interesting to use BLI to reveal whether such barriers prevent initial or propagated HSC foci. Thus, the strategy described here will provide a basis for elucidating the molecular and cellular processes that contribute to successful hematopoietic engraftment and for identifying the homing and microenvironmental requirements in this process.

We thank S. Smith for antibody production. This work was supported in part by unrestricted gifts from the Mary L. Johnson and Hess Research Funds (to C.H.C.); National Institutes of Health Grants RO1DK58664, R33CA88303, R24CA92862, P20CA86312 (to C.H.C.), CA86065 (to I.L.W.), and P01CA49605 (to C.H.C., R.S.N., and I.L.W.); and the Frederick Frank/Lehman Brothers, Inc., Irvington Institute Fellowship (to A.J.W.).

1. Spangrude, G. J., Heimfeld, S. & Weissman, I. L. (1988) *Science* **241,** 58–62.
2. Morrison, S. J. & Weissman, I. L. (1994) *Immunity* **1,** 661–673.
3. Aizawa, S. & Tavassoli, M. (1988) *Proc. Natl. Acad. Sci. USA* **85,** 3180–3183.
4. Hardy, C. L. (1995) *Am. J. Med. Sci.* **309,** 260–266.
5. Hendrikx, P. J., Martens, C. M., Hagenbeek, A., Keij, J. F. & Visser, J. W. (1996) *Exp. Hematol. (Charlottesville, Va)* **24,** 129–140.
6. Quesenberry, P. J. & Becker, P. S. (1998) *Proc. Natl. Acad. Sci. USA* **95,** 15155–15157.
7. Cui, J., Wahl, R. L., Shen, T., Fisher, S. J., Recker, E., Ginsburg, D. & Long, M. W. (1999) *Br. J. Haematol.* **107,** 895–902.
8. Szilvassy, S. J., Bass, M. J., Van Zant, G. & Grimes, B. (1999) *Blood* **93,** 1557–1566.
9. Contag, P. R., Olomu, I. N., Stevenson, D. K. & Contag, C. H. (1998) *Nat. Med.* **4,** 245–247.
10. Sweeney, T. J., Mailander, V., Tucker, A. A., Olomu, A. B., Zhang, W., Cao, Y.-A., Negrin, R. S. & Contag, C. H. (1999) *Proc. Natl. Acad. Sci. USA* **96,** 12044–12049.
11. Edinger, M., Sweeney, T. J., Tucker, A. A., Olomu, A. B., Negrin, R. S. & Contag, C. H. (1999) *Neoplasia* **1,** 303–310.
12. Edinger, M., Cao, Y.-A., Verneris, M. R., Bachmann, M. H., Contag, C. H. & Negrin, R. S. (2003) *Blood* **101,** 640–648.
13. Wagers, A. J., Sherwood, R. I., Christensen, J. L. & Weissman, I. L. (2002) *Science* **297,** 2256–2259.
14. Morrison, S. J., Wandycz, A. M., Hemmati, H. D., Wright, D. E. & Weissman, I. L. (1997) *Development (Cambridge, U.K.)* **124,** 1929–1939.
15. Christensen, J. L. & Weissman, I. L. (2001) *Proc. Natl. Acad. Sci. USA.* **98,** 14541–14546.
16. Wright, D. E., Cheshier, S. H., Wagers, A. J., Randall, T. D., Christensen, J. L. & Weissman, I. L. (2001) *Blood* **97,** 2278–2285.
17. Smith, L. H. & Clayton, M. L. (1970) *Exp. Hematol. (Charlottesville, Va)* **20,** 82–84.
18. Wang, X., Rosol, M., Ge, S., Peterson, D., McNamara, G., Pollack, H., Kohn, D. B., Nelson, M. D. & Crooks, G. M. (2003) *Blood* **102,** 3478–3482.
19. Muller-Sieburg, C. E. & Riblet, R. (1996) *J. Exp. Med.* **183,** 1141–1150.
20. Morrison, S. J., Qian, D., Jerabek, L., Thiel, B. A., Park, I. K., Ford, P. S., Kiel, M. J., Schork, N. J., Weissman, I. L. & Clarke, M. F. (2002) *J. Immunol.* **168,** 635–642.
21. Shizuru, J. A., Jerabek, L., Edwards, C. T. & Weissman, I. L. (1996) *Biol. Blood Marrow Transplant.* **2,** 3–14.
22. Aguila, H. L. & Weissman, I. L. (1996) *Blood* **87,** 1225–1231.